Available online at www.sciencedirect.com

SciVerse ScienceDirect

Ceramics International 38 (2012) 4057–4064

CERAMICS INTERNATIONAL

www.elsevier.com/locate/ceramint

Effects of humidity on titania-based polyvinylpyrolidone (PVP) electrospun fibers

Nishant M. Tikekar *, John J. Lannutti

Department of Materials Science and Engineering, 448 MacQuigg Labs, 105W Woodruff Avenue, Ohio State University, OH 43210, USA

Received 8 December 2011; received in revised form 23 January 2012; accepted 24 January 2012
Available online 31 January 2012

Abstract

Humidity effects on titania-based nanofibers were studied by electrospinning solutions of different weight percentages of titanium (IV) *n*-butoxide (TNBT) and polyvinylpyrolidone (PVP) in *N*,*N*-dimethylformamide (DMF). Ambient humidities during electrospinning were typically varied between 25 and 75% RH. XRD and SEM were used to examine crystallization and determine optimal conditions for fiber formation. A specific combination of solute concentration (45–55 wt%) and ambient humidity (25–60% RH) allowed fiber formation. Lower solute concentrations resulted in electrospraying while higher humidities induced excessive plasticization of the PVP. Using a heated target allowed fiber formation at higher humidities (>60%). Following electrospinning, slight degradation of the 60 wt% (but not the 50 wt%) TNBT microstructure was observed when stored for longer periods possibly due to higher moisture uptake in case of higher solids loading. Examination of the fibers following pyrolysis at 500 °C for 6 h in air revealed the presence of individual nanoscale crystallites that could potentially boost ionic and electronic diffusion in batteries and solar applications.

Keywords: B. Fibers; B. Nanocomposites; D. TiO_2

1. Introduction

Titania is a wide band-gap semi-conducting ceramic having potential uses in many applications including photocatalysis and solar cells for power generation [1–5]. Although two common crystalline forms – rutile and anatase – exist, it is the anatase form that exhibits activity in photocatalysis and solar applications [6]. Natural sunlight as well as dye-based light sensitizers cause electrons to jump from the valence band to the conduction band in anatase titania, thus creating positive holes in the valence band. This phenomenon is termed charge separation in solar cells and the separated charges can lead to the generation of electricity [1–3]. The photo-voltaic performance and photo-catalytic efficiency of the anatase titania are strongly influenced by the specific surface area and overall morphology of the titania phase.

Electrospinning is a fabrication technique that utilizes electrostatic repulsion to create fine submicron-scale or nano-scale fibers. Besides being a simple technique for fiber formation, a key advantage is its ability to form nano-diameter fibers having high specific surface areas. Numerous electrospun ceramic nanofibers, including silica (SiO_2) and titania (TiO_2), have been fabricated by this process [6–12]. Additionally, lithium manganate (LMO) and lithium titanate (LTO) based electrospun fibers are being investigated for lithium-ion battery applications [13]. In such applications, these fibers essentially act as high surface area pathways for ionic and electronic diffusion, thus enhancing battery efficiency. TiO_2 fibers are of particular interest because of the many precursors from which they can be easily electrospun [6–12,14].

Typically, the titania-based spin dopes can be classified into two types, namely, (1) alkoxide precursors such as titanium (IV) *n*-butoxide (TNBT), and (2) organic solutions containing alkoxide precursors and a carrier polymer such as polyvinyl-pyrolidone (PVP). The ability to form fibers upon electrospinning can be influenced by a number of factors such as pH, viscosity, molecular weights and the relative concentrations of the components in the solution. If the viscosity is too low, beaded fibers form and are typically undesirable. Alternatively, if the solution is too viscous, electrospinning itself becomes

* Corresponding author at: Watts Hall, 2041 College Rd., Columbus, OH 43210, USA. Tel.: +1 614 292 3926; fax: +1 614 292 3926.
E-mail address: tikekar.2@osu.edu (N.M. Tikekar).

0272-8842/$36.00
doi:10.1016/j.ceramint.2012.01.063

difficult [15,16]. Precursors with good solubility in organic solvents are relatively easily manageable in terms of altering their viscosities and thus allowing the production of fibers by electrospinning. Uniform, non-beaded fibers can be spun and, hence these types of spin dopes are widely adopted [8,17].

Polyvinylpyrolidone (PVP) is a widely used carrier polymer allowing the electrospinning of ceramics [13,18,19]. However, PVP has considerable affinity for moisture. High humidity could plasticize as-spun fibers hindering retention of the desired electrospun morphology. An additional objective of this study was to investigate the effects of different humidity conditions as well as composition and ratios of the precursor components. Finally, the general effects of pyrolysis on fiber structure and final oxide crystallinity were also observed.

2. Experimental

2.1. Materials

Titanium (IV) *n*-butoxide (TNBT, 97%, Sigma–Aldrich 244112), polyvinylpyrolidone (PVP, Sigma–Aldrich PVP 360, M_W = 360,000), *N*,*N*-dimethylformamide (DMF, ≥99.8%, Sigma–Aldrich 319937) and acetic acid (>99.85%, glacial, Sigma–Aldrich 695084) were obtained and used without further purification.

2.2. Spin dopes

All the spin dopes were prepared by dissolving the solutes at the desired ratio in DMF at 75 °C for 2 h. After cooling to room temperature, the solutions were electrospun using conditions described in the next section. Spin dopes were prepared with various concentrations of TNBT + PVP in DMF. TNBT: PVP ratio was maintained at 1:1 by vol% in all the experiments. The weight percentages studied initially were in the range of 6–18 wt%. These solutions resulted in spraying and hence the TNBT + PVP contents were increased progressively from 30 to 70 wt%. The 30 and 40 wt% solutions resulted mostly in spraying; however, some fibers were observed within the film.

Table 1 shows the compositions yielding electrospun fiber and the ambient conditions used to examine the effects of humidity. The experiments were desgined based on the modified Taguchi L9 experimental design [20]. The wt% reflects the total percentage of TNBT + PVP in the solution. A small amount (∼2 wt%) of acetic acid (HAc) was added to all the solutions to control potential hydrolysis/gelation of TNBT [6]. Samples with 50–70 wt% solids content were spun at 25, 50 and 75% RH.

2.3. Electrospinning

Electrospinning was conducted using a syringe pump in a humidity chamber that allowed controlled humidity conditions. In each experiment, electrospinning occurred using a voltage of +17 kV and a flow rate of 2 ml/h. The syringe used was BD 20 ml Syringe with Luer-Lok Tip. The diameter of the needle tip was 0.91 mm. The distance between the syringe and the collector (target) was 20 cm [21]. The electrospun fiber was collected on aluminum foil wrapped on a steel target. For this study, an enclosure (a plastic chamber) of dimensions $48'' \times 36'' \times 30''$ was built to allow electrospinning under conditions of controlled humidity. Small holes of ∼0.5″ diameter acted as gas inlet and outlet. Humidity levels ≤75% in the box were maintained using a controlled N_2 gas flow. Higher humidity (∼100%) could be achieved by evaporating water from a beaker on a hot plate placed inside the chamber. One side of the box had a sealable plastic door through which it was possible to transfer the electrospinning equipment. The other side of the box had a couple of large circular inlets to which were attached rubber gloves. This allowed access to the user to attend to the processes inside the box while controlled humidity conditions were maintained. Fig. 1(a and b) is photographs of the enclosure and the electrospinning setup within the plastic chamber.

In addition, 70 wt% TNBT + PVP solution spun at humidity levels of >60% (high humidity) was spun on a hot plate at 120, 200 and 300 °C. Electrospun fibers of different wt% were then pyrolyzed in a Carbolite CWF 1200 furnace at 500 °C for 6 h. The heating rate from the room temperature to 500 °C was 2 °C/m and the samples were cooled overnight inside the furnace in ambient conditions. XRD was conducted using a Rigaku Ultima III XRD and the electrospun and pyrolyzed fibers coated with Au were examined using a Sirion high-resolution field-emission gun scanning electron microscope (SEM). XRD was conducted for 2 theta ranging from 20 to 60°. The step size during XRD was 0.02° and time per step was 2 s. The samples were coated with Au under 10^{-1} mbar at 10 mA pressure for 60 s.

Table 1
Experimental conditions and resulting fiber diameters following electrospinning TNBT + PVP dissolved in DMF.

Experiment #	Total (TNBT + PVP) wt% in DMF	Humidity (%)	Average diameter (μm)
1	50	25	1.15 ± 0.32
2	50	50	1.32 ± 0.35
3	50	75/ambient	0.92 ± 0.21
4	60	75/ambient	17.58 ± 10.73
5	60	25	1.81 ± 0.41
6	60	50	1.52 ± 0.49
7	70	50	1.40 ± 0.46
8	70	75/ambient	Film formed
9	70	25	1.84 ± 1.07

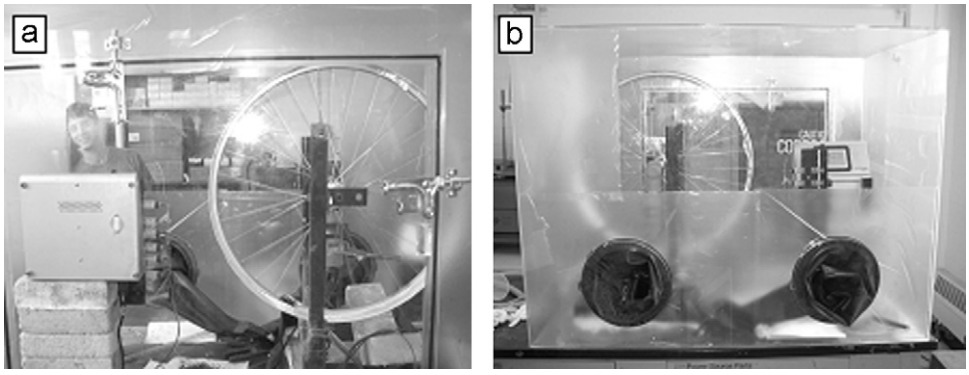

Fig. 1. (a and b) Images of the humidity chamber containing the electrospinning equipment.

3. Results and discussion

3.1. Electrospinning in the humidity chamber

Initially, TNBT + PVP in DMF compositions between 6 and 18 wt% were electrospun at 17 kV and a flow rate of 2 ml/h. In contrast to the observations of Chandrasekhar et al. [6], none of these solutions resulted in a clean fibrous structure as can be seen in SEM images of these compositions in Fig. 2(a–d). Almost all solutions resulted in electrospraying even at low levels of humidity (25% RH). However, as seen in Fig. 2(d), in case of the 18 wt% TNBT + PVP solution, some fibers are visible within the electro-sprayed bead-like mat at higher magnification. This suggested that higher solute contents could lead to higher viscosities and potentially result in the desired fiber structure. The solute content was thus sequentially increased until fiber was uniformly obtained at low humidity levels (25% RH). Fig. 3(a and b) is SEM images of samples electrospun at 25% RH from solutions containing 30 and 40 wt% TNBT + PVP solutions, respectively. Clearly, as the solute content increases, the fiber content of the electrospun deposition also correspondingly increases. However, as the images show, majority of the deposition was film-like and displayed only a very few fibers.

The composition was then varied between 50 and 70 wt% and fibers were electrospun at 25, 50 and 75% RH to determine the effects of humidity on these higher wt% TNBT + PVP compositions. The objective was to determine if higher solute concentrations resulted in fiber structure upon electrospinning. Fig. 4(a–c) is the SEM images of samples electrospun from 50 wt% TNBT + PVP solutions at 25, 50 and 75% RH. Clean fiber structure without beading formed within the electrospun

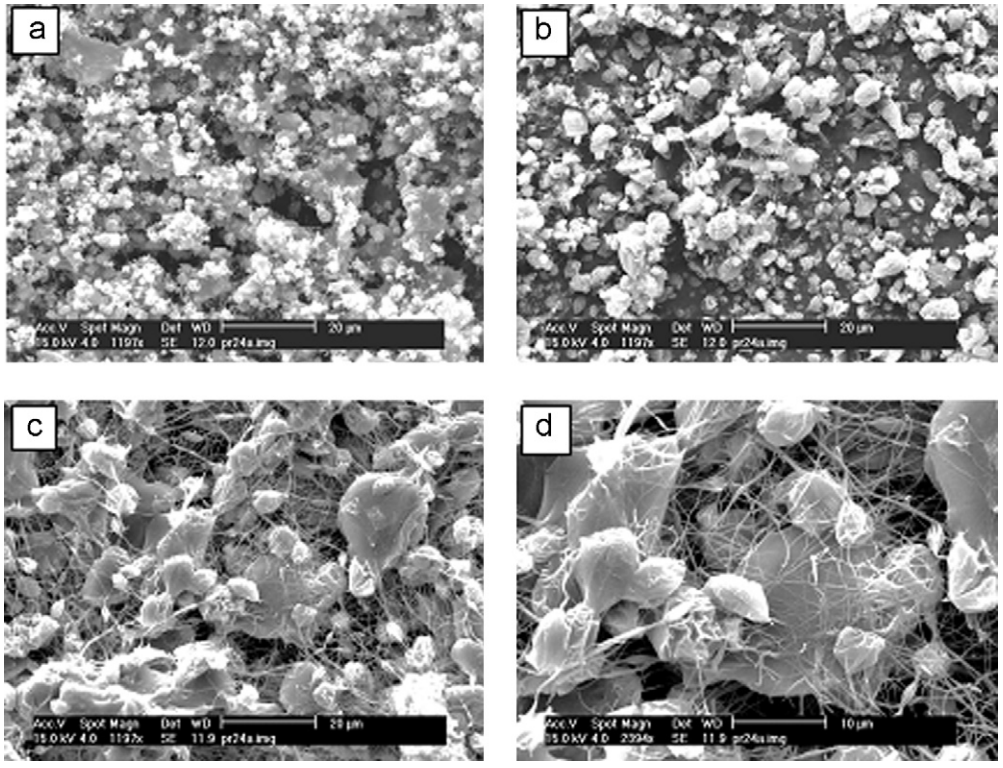

Fig. 2. SEM images of as-spun 6 and 12 wt% TNBT + PVP + DMF (a and b) and 18 wt% TNBT + PVP + DMF (c and d) samples at humidity levels of 25% RH.

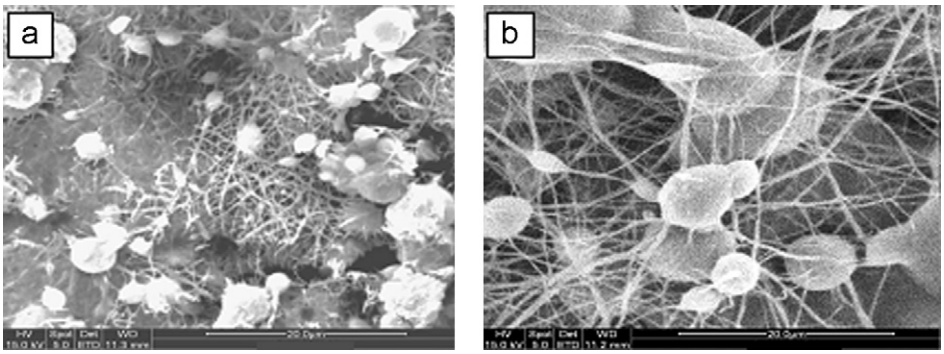

Fig. 3. SEM images of as-spun (a) 30 wt% and (b) 40 wt% TNBT + PVP + DMF samples spun at humidity levels of 25% RH.

sheets regardless of humidity. Thus, 50 wt% seems to be the minimal solute content necessary for fiber retention in spite of electrospinning exposures to the higher ambient humidity (75% RH). Fig. 4(d–f) is the SEM images of samples electrospun from solutions containing 60 wt% TNBT + PVP solutions at 25, 50 and 75% RH. While clean fibrous structure was found to have formed within the electrospun sheet at 25 and 50% RH, at 75% RH PVP plasticization likely drives large changes in diameter and fiber–fiber bonding [21]. In contrast to the 50 wt% result, higher humidity levels for a solution with 60 wt% TNBT + PVP in DMF appear detrimental to these relatively higher solute contents. Average fiber diameters are provided in Table 1.

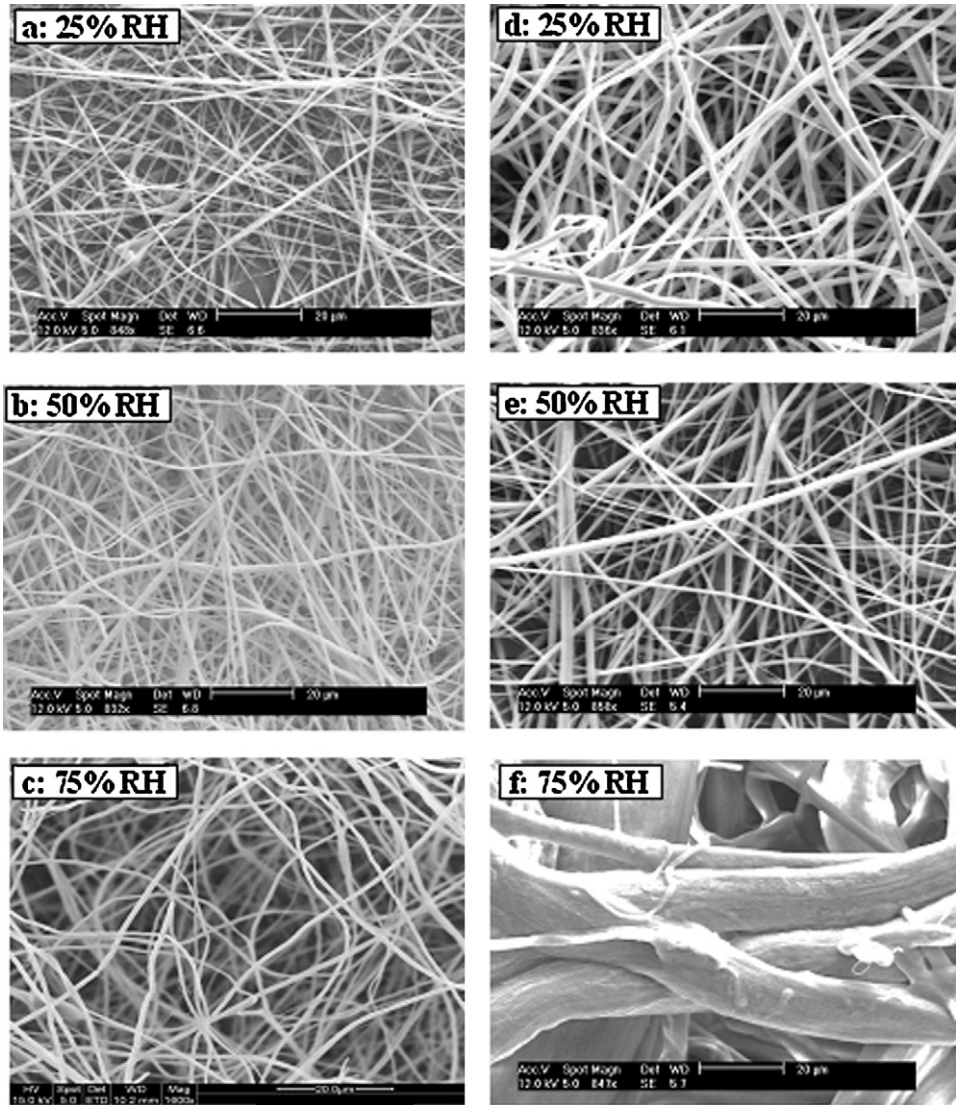

Fig. 4. SEM images of as-spun 50 wt% TNBT + PVP + DMF (a–c) and 60 wt% TNBT + PVP + DMF (d–f) spun at the given humidity levels.

No significant difference in average diameter for most of the conditions was found. Solutions containing 60 wt% TNBT + PVP spun at 75% RH resulted in relatively large fiber diameters because the electrospun fiber was evolving toward a film due to the high humidity. The electrospun deposit evolved completely into a film in the case of 70 wt% TNBT + PVP spun at 75% RH.

Clearly, a favorable window appears to exist in which a combination of wt% solute and humidity levels provide appropriate electrospinning conditions. Potentially, a combination of higher wt% solute and higher humidity could destabilize the jet and result in electrospraying. Solutions at 70 wt% TNBT + PVP were electrospun to investigate this possibility. Fig. 5(a–c) shows deposits formed from the 70 wt% TNBT + PVP in DMF electrospun at 25, 50 and 75% RH. While the sample spun at 25% RH resulted in at least some fiber structure, samples spun at higher humidity tended toward a film-like morphology. The average diameter of the sample spun at 25% RH was 1.84 ± 1.07 μm and that spun at 50% RH was 1.40 ± 0.46 μm. These values are not significantly different from samples containing 50 wt% and 60 wt% electrospun under similar humidity conditions.

3.2. Electrospinning on a high temperature target

Experiments were conducted to determine whether a hot target could decrease the influence of humidity on electrospun fiber. Fig. 5(d–f) is SEM images of 70 wt% TNBT + PVP solution electrospun in higher ambient humidity (>70% RH) on an aluminum foil-wrapped hot plate at temperatures of 120, 200 and 300 °C. Fibers spun on the target at 120 and 200 °C resulted in a clean fiber structure resembling the structure observed at room temperature in 25% RH. The average diameters of the fibers spun at 120 and 200 °C were 1.48 ± 0.41 μm and 1.67 ± 0.40 μm respectively. Electrospinning on a target maintained at 300 °C also resulted in fiber structure and an average diameter of 2.28 ± 1.26 μm. However, the fibers were broken/discontinuous and exhibited wide variations in diameter. A target temperature of 300 °C may be too high to fabricate a fiber sheet composed of interconnected, continuous fibers. This could cause rapid melting of PVP as the fiber is being deposited on the hot plate, leading to shrinkage and cracking of the fiber. As seen in Fig. 5(g), when the sample is spun on the hot target (300 °C) under very humid conditions, the fibers are fragmented and the deposition appears to be forming a non-fibrous film. As areas of fiber shrink, it could lead to cracking caused by the shrinkage of adjacent fiber areas away from each other. A high magnification image [inset in Fig. 5(f)] of the sample at 300 °C reveals individual nano-size grains/crystallites within the fiber, suggesting that pyrolysis has begun in earnest.

Electrospun samples were then pyrolyzed at 500 °C for 6 h in air using a heating rate of 2 °C/min. Fig. 6(a–d) is the

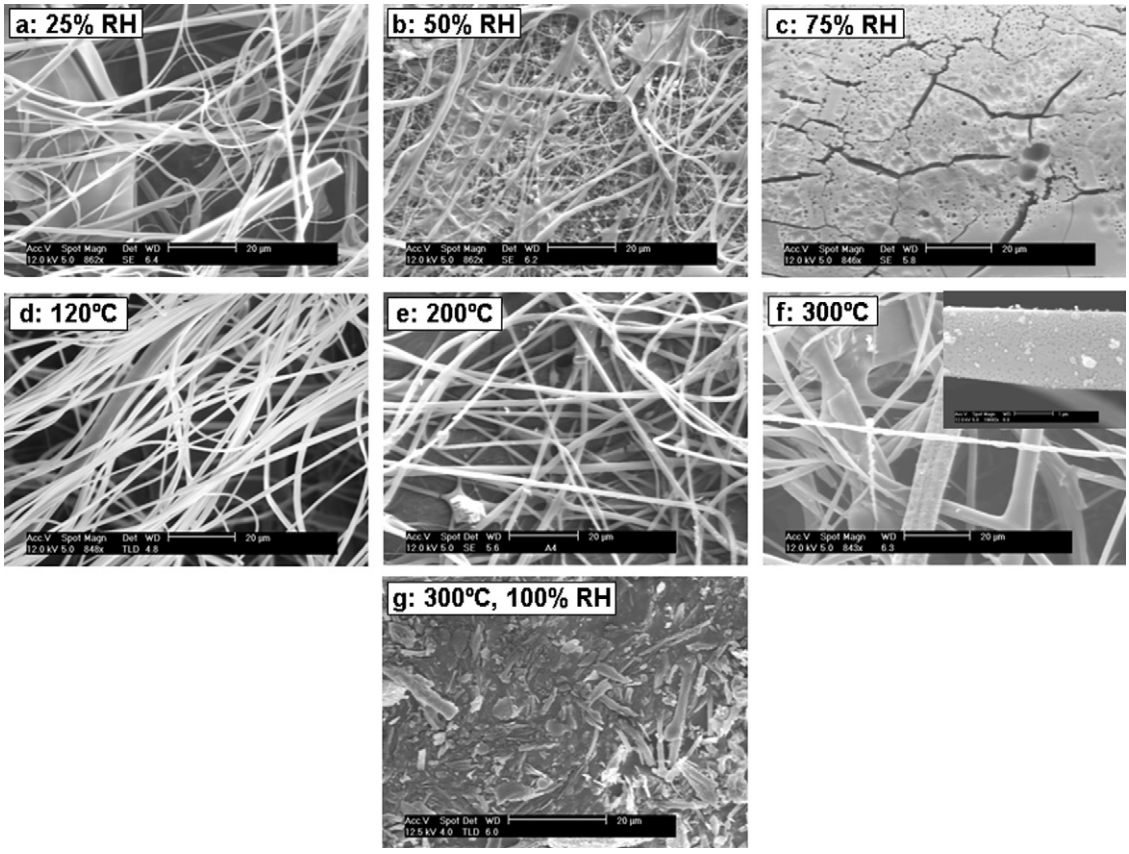

Fig. 5. SEM images of as-spun 70 wt% TNBT + PVP + DMF spun at different humidity conditions (a: 25% RH, b: 50% RH, c: 75% RH) and on a hot plate at higher temperatures (d: 120 °C, e: 200 °C, f: 300 °C) in ambient humidity (>70% RH). SEM image (g) of sample spun on hot plate (300 °C) in 100% RH.

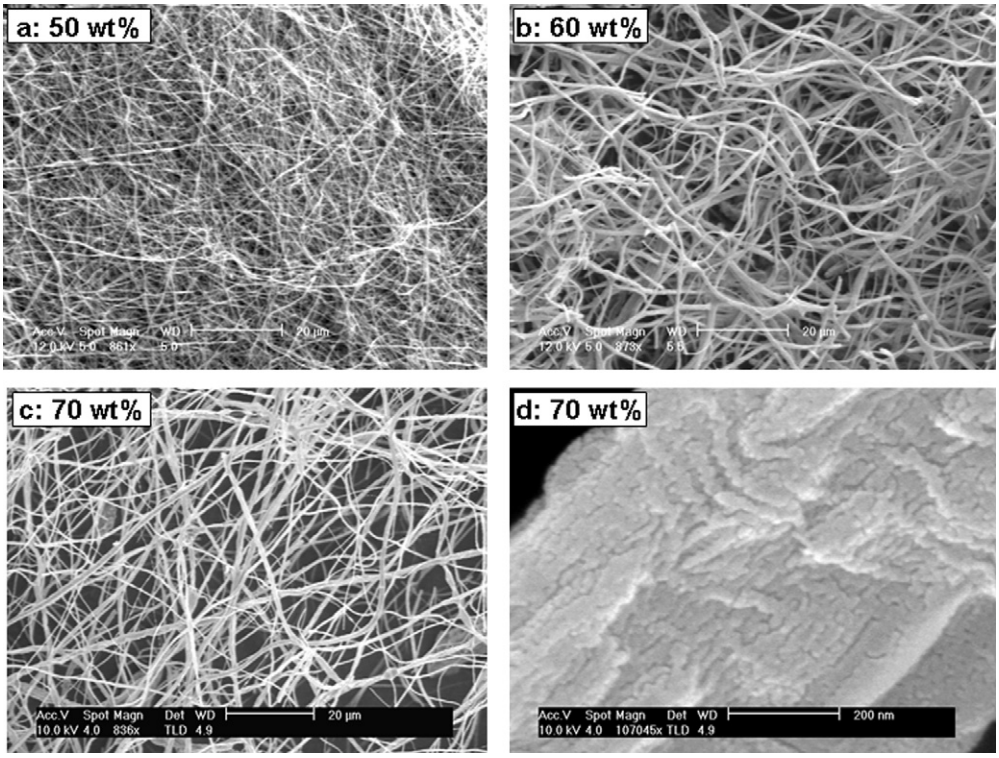

Fig. 6. SEM images of (a) 50 wt%, (b) 60 wt%, (c and d) 70 wt% TNBT + PVP + DMF pyrolyzed at 500 °C for 6 h in air.

SEM images of the pyrolyzed samples of different compositions. If the initial as-spun structure is fiber-based, fiber structure is retained even after pyrolysis. Additionally, high magnification [Fig. 6(d)] revealed the individual crystallites making up the fiber structure and had an average crystallite size of ~10 nm. The average diameters of the pyrolyzed fibers were 0.63 ± 0.13 μm for the 50 wt% sample, 1.00 ± 0.25 μm for the 60 wt% sample and 1.03 ± 0.33 μm for the 70 wt% sample. Although slightly lesser than the as-spun samples, the fibers had not shrunk significantly in diameter. Fig. 7 depicts XRD patterns generated by the different samples (50–70 wt%) following pyrolysis. The diffraction patterns matched those of anatase-phased TiO_2 and revealed that the inter-planar spacing of all TiO_2 grains was <100 nm. Compared to the XRD peaks of a commercially obtained TiO_2 powder, the peaks generated by these fibers were broader. According to the Scherrer equation [22], this suggests that the average size of the single-crystalline grains in the electrospun TiO_2 fibers was significantly smaller and close to 10 nm. It is expected that such nanoscale grains could result in high grain boundary diffusion to enhance the conductivity of solar cells.

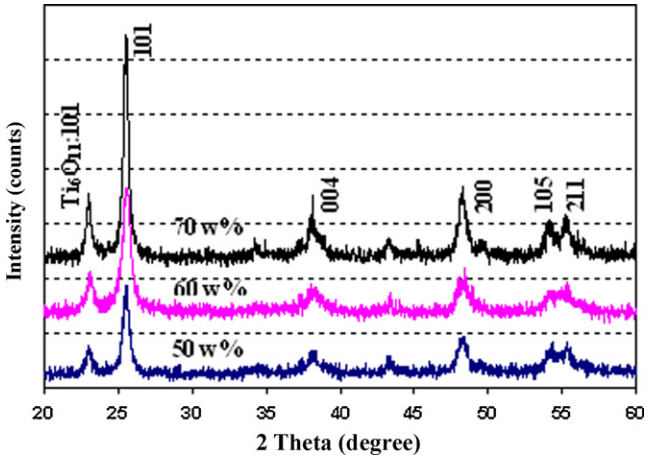

Fig. 7. XRD patterns of the electrospun samples following pyrolysis.

3.3. Exposure to high ambient humidity (≥70% RH) and storage

Sheets electrospun using 50 and 60 wt% TNBT + PVP solution at humidities of 25% RH were exposed to ambient humidity (~75% RH) for periods up to 96 h to determine if their structure could withstand exposure to high humidity for long periods. Fig. 8(a and b) is the respective SEM images of 50 and 60 wt% TNBT + PVP samples exposed to ambient humidity (~75% RH). In both the sheets, fiber structure was largely retained even after extended exposure to these high levels of ambient humidity. The average diameter of the 50 wt% sample was 1.16 ± 0.38 μm and the 60 wt% sample was 1.12 ± 0.55 μm. However, degradation of the 60 wt% TNBT microstructure was observed. The 50 wt% TNBT microstructure showed no signs of similar degradation. This suggests that a connection between solids loading and microstructural instability exists that potentially increases moisture uptake.

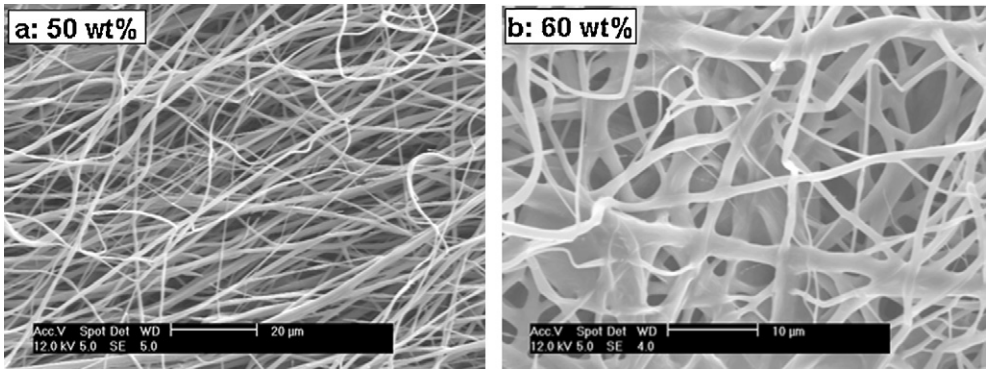

Fig. 8. SEM images of as-spun (a) 50 wt% and (b) 60 wt% spun at 25% RH after exposure to ∼75% RH for 96 h.

3.4. Rationale for fiber formation

A window of conditions that allow fiber formation based on a combination of solute content and ambient humidity was identified. Any extreme in either of these conditions inhibits fiber formation and results in a film-like deposition. Low solute content clearly hinders fiber formation. High humidity allows for fiber formation but the sample deforms and evolves into a film for samples with high solute content. Samples with low solute contents (50 wt% TNBT + PVP) are however, able to retain the fiber structure even at higher humidities.

4. Conclusions

In this study, titania fibers were fabricated using titania-based (TNBT + PVP + DMF) precursors. Effects of solid content and humidity levels on the formation and durability of the fiber structure were investigated. A minimum solute content of 45–55 wt% was necessary for fiber formation without electrospraying or excessive beading. Solutions containing 50 wt% TNBT + PVP were spun into nano-sized fibers at all the humidity levels studied. When spun at higher (75% RH) humidity levels, solutions with higher TNBT + PVP content (60 and 70 wt%) appeared to result in plasticization and loss of fiber structure. This indicates the existence of a ''favorable window'' in which 45–60 wt% TNBT + PVP may be electrospun at all three humidity levels. Electrospinning onto a hot target at temperatures >100 °C resulted in fiber structure even at higher humidity levels (>70%). Pyrolyzing the fibers at 500 °C for 6 h revealed nano-size crystallites that could potentially enhance grain boundary diffusion and thus the performance in solar cells. Future investigation should include electrospinning aligned titania nanofibers to test for applications as electrodes for solar cells.

Acknowledgments

This material is based upon work supported by the National Science Foundation Grant Nos. IIP-0930626 and EEC-0425626. Any opinions, findings, and conclusions or recommendations expressed in this material are those of the authors and do not reflect the views of the National Science Foundation.

References

[1] G. Yu, J. Gao, J.C. Hummelen, F. Wudl, A.J. Heeger, Polymer photovoltaic cells—enhanced efficiencies via a network of internal donor-accepted heterojunctions, Science 270 (1995) 1789.
[2] U. Bach, D. Lupo, P. Comte, J.E. Moser, F. Weissorte, J. Salbeck, H. Spreitzer, M. Gratzel, Solid-state dye-sensitized mesoporous TiO_2 solar cells with photon to electron conversion efficiencies, Nature 395 (1999) 583.
[3] C.J. Brabec, N.S. Sariciftci, J.C. Hummelen, Plastic solar cells, Advanced Functional Materials 11 (2001) 15.
[4] A. Wold, Photocatalytic properties of TiO_2, Chemistry of Materials 5 (1993) 280.
[5] M.R. Hoffman, S.T. Martin, W. Choi, D.W. Bahnemann, Environmental applications of semiconductor photocatalysis, Chemical Reviews 95 (1995) 69.
[6] R. Chandrasekar, L.F. Zhang, J.Y. Howe, N.E. Hedin, Y. Zhang, H. Fong, Fabrication and characterization of electrospun titania nanofibers, Journal of Materials Science 44 (2009) 1198.
[7] S.S. Choi, S.G. Lee, S.S. Im, S.H. Kim, Y.L. Joo, Silica nanofibers from electrospinning/sol–gel process, Journal of Materials Science Letters 22 (2003) 891.
[8] Y. Liu, S. Sagi, R. Chandrasekar, L.F. Zhang, N.E. Hedin, H. Fong, Preparation and characterization of electrospun SiO_2 nanofibers, Journal of Nanoscience and Nanotechnology 8 (2008) 1528.
[9] D. Li, J.T. McCann, M. Gratt, Y.N. Xia, Photocatalytic deposition of gold nanoparticles on electrospun nanofibers of titania, Chemical Physics Letters 394 (2004) 387.
[10] D. Li, Y.N. Xia, Fabrication of titania nanofibers by electrospinning, Nano Letters 3 (2003) 555.
[11] S.H. Lee, C. Tekmen, W.M. Sigmund, Three-point bending of electrospun TiO_2 nanofibers, Materials Science and Engineering A 398 (2005) 77.
[12] W. Nuansing, S. Ninmuang, W. Jarernboon, S. Maensiri, S. Seraphin, Structural characterization and morphology of electrospun TiO_2 nanofibers, Materials Science and Engineering B 131 (2006) 147.
[13] N.M. Tikekar, J.J. Lannutti, R. Revur, S. Sengupta, Journal of New Materials for Electrochemical Systems, in press.
[14] S.K. Choi, S. Kim, S.K. Lim, H.H. Park, Photocatalytic comparison of TiO_2 nanoparticles and electrospun TiO_2 nanofibers: effects of mesoporosity and interparticle charge transfer, Journal of Physical Chemistry C 114 (2010) 16475.
[15] C.J. Thompson, G.G. Chase, A.L. Yarin, D.H. Reneker, Effects of parameters on nanofiber diameter determined from electrospinning model, Polymer 48 (2007) 6913.
[16] H. Fong, I. Chun, D.H. Reneker, Beaded nanofibers formed during electrospinning, Polymer 40 (1999) 4585.
[17] S.A. Theron, E. Zussman, A.L. Yarin, Experimental investigation of the governing parameters in the electrospinning of polymer solutions, Polymer 45 (2004) 2017.

[18] Z.Y. Cai, J.S. Li, Y.G. Wang, Fabrication of zinc titanate nanofibers by electrospinning technique, Journal of Alloys and Compounds 489 (2010) 167.
[19] S. Maensiri, W. Nuansing, J. Klinkaewnarong, P. Laokul, J. Khemprasit, Nanofibers of barium strontium titanate (BST) by sol–gel processing and electrospinning, Journal of Colloid and Interface Science 297 (2006) 578.
[20] R.K. Roy, A Primer on the Taguchi Method, 1st ed., Society of Manufacturing Engineers, 1990.
[21] J. Gaumer, A. Prasad, D. Lee, J.J. Lannutti, Structure–function relationships and source-to-ground distance in electrospun polycaprolactone, Acta Biomaterialia 5 (2009) 1552.
[22] L.E. Alexander, X-ray diffraction methods in polymer science, 1st ed., John Wiley and Sons Inc., 1969, pp. 423, 582.